TECHNICAL PAPER

Statistical analysis of the uniformity of sprays of tire pyrolysis oil-diesel oil blends

Alexander A. R. Gamboa[1,4] · Leila R. dos Santos[1] · Cristiane A. Martins[1] · German R. A. Chumpitaz[2] · José C. de Andrade[3] · João A. de Carvalho Jr[4]

Abstract

Tire pyrolysis oil (TPO) shows promise as alternative fuels, not only for the raw material from which they can be produced (waste tires), but also their physical characteristics. In this work, the atomisation quality of TPO and its blends with diesel oil was evaluated from a statistical perspective. A 35 kW Y-jet atomiser, operating at an air-fuel mass ratio (AFR) in the range of 0.075 to 0.150, was used to produce the fuel sprays. The Log-Normal density function was used to describe the droplet size distribution of the sprays. Additionally, the d^2-law was integrated into the density function to simulate TPO spray evaporation. The results showed that the increase in TPO in the fuel blend decreased the uniformity of droplet sizes in the spray, as well as increased the presence of larger droplets. However, operating the atomiser at a AFR = 0.150 reduced the presence of larger droplets and increased the volume fractions of smaller droplets.

Keywords Atomisation · Spray · Tire pyrolysis oil · Droplet size distribution

List of symbols

AFR	Air-fuel mass ratio
DO	Diesel oil
f	Density function
FO	Fuel oil
K	Burning rate coefficient, mm^2/s
t	Time, s
TPO	Tire pyrolysis oil
V	Volume fraction
W	Mass fraction
W_{evap}	Mass fraction of vapour formed
x	Diameter, μm
x_{32}	Sauter mean diameter, μm
x_{MMD}	Mass median diameter, μm
y	Dimensionless variable
δ	Uniformity parameter

✉ Alexander A. R. Gamboa
  alexander.r.gamboa@gmail.com

1   Combustion, Propulsion and Energy Laboratory, Technological Institute of Aeronautics, Rod. Praça Marechal Eduardo Gomes, 50, São José dos Campos, São Paulo 12228-900, Brazil

2   Mechanical Engineering Institute, Federal University of Itajubá, Ave. BPS, 1303, Itajubá, Minas Gerais 37500-903, Brazil

3   Combustion and Propulsion Laboratory, National Space Research Institute, Rod. Press. Dutra, km 39, Cachoeira Paulista, São Paulo 12630-000, Brazil

4   Energy Department, São Paulo State University, Av. Ariberto P. Cunha, 333, Guaratinguetá, São Paulo 12510-410, Brazil

1 Introduction

The production of waste tires brings with it the responsibility to dispose of them properly, aiming for the least impact on the environment. According to the World Business Council for Sustainable Development (WBCSD), in its 2019 report, approximately 30.9 million tonnes of waste tires were produced in countries covering 89% of the world's vehicle fleet, with China being the largest producer (~47%) [1]. In 2020, approximately 670 thousand tonnes of tires were sold in Brazil, of which 98.52% were collected as waste. The scrap tires collected in Brazil are appropriately destined using the technologies in force (co-processing, lamination, granulation, and pyrolysis), with co-processing (62.10%) being the main destination, while pyrolysis represents only 0.98% [2].

One of the main disadvantages of using tires directly as fuel is the difficulty of burning them compared to a liquid or gaseous fuel. In tire pyrolysis, 63.3, 24.8 and 11.9 mass

percent of the tire's sulphur is distributed among the solid, liquid and gaseous products, respectively [3]. The solid product of pyrolysis corresponds to the tire residue after the loss of its volatile components during thermal degradation in an anoxic environment, while the liquid and gaseous product results from the cooling of the released vapours to environmental temperature. The volatile content of the tire can range from 58.76 to 62% of its original mass [4–6], while plant biomass can contain between 63.8 and 77% [7, 8]. Although plant biomass has a higher volatile content than tires, the literature indicates [3, 9–11] that the energy content of tire pyrolysis products (gas and liquid) is higher.

Of the products of tire pyrolysis, the liquid product known as tire pyrolysis oil (TPO), is particularly attractive for use as a fuel because it has a viscosity (5.43 cSt) [6], density (921 kg/m^3) [3], surface tension (0.028 N/m) [12], and high heating value (46.32 MJ/kg) [13] similar to diesel oil. These physical properties have motivated research into its application in furnaces [14], boilers [15], and compression ignition engines [6, 13], as well as theoretical evaluations in various combustion systems [16]. Generally, TPO is blended with diesel or biodiesel to reduce the sulphur content and improve the cetane number of the fuel blend [17, 18]. However, the evaluation of the quality and applicability of TPO has mainly focussed on combustion emissions and the performance of thermal plants using this fuel (and blends with diesel/biodiesel), ignoring the atomisation process, which is directly related to combustion efficiency. To illustrate the lack of work on the processes preceding the combustion of TPO, i.e. the generation of fuel mist(atomisation) and the evaporation of the droplet distribution, a search with different word combinations in the Scopus database is shown in Fig. 1.

As can be seen in Fig. 1, the keywords included the generic word "combustion" which was combined with "spray", "atomisation", "droplet" and "evaporation". Subsequently, the words "alternative fuel", "pyrolysis/pyrolytic oil AND tire" were added to compare knowledge production in the area of pre-combustion processes of TPO and other alternative fuels. The numbers in parentheses indicate the number of documents for the word combinations corresponding to the base year 1976 to 2021. For example, combining the words "combustion", "evaporation" and "pyrolysis/pyrolytic oil" resulted in a total of 21 documents. Based on Fig. 1, a growing trend in the number of published documents can also be observed, which shows that the combustion processes to date are of great interest in the scientific community, especially in the field of alternative fuels, as a deepening of their knowledge makes it possible to know the advantages and limitations when used as a substitute for conventional fuels (fossil and depletable) in combustion equipment. The data show that research on the atomisation and evaporation of TPO is still scarce, with only 5, 3, 4 and 2 documents found for the keywords "spray", "atomisation",

"droplet" and "evaporation", respectively. Of the documents identified for TPO, the articles by Chumpitaz et al. [12], Williams et al. [14], and Muelas et al. [19] focused on the study of atomisation and evaporation of TPO and blends with diesel oil, while the other papers [20, 21], in discussing their results, used the quality of atomisation (droplet size) and evaporation of TPO to justify the data obtained, but did not perform measurements of droplet size, evaporation or droplet size distribution.

Muelas et al. [19] investigated the combustion characteristics of TPO using a drop tube system and evaluated the evolution of droplet and flame size, burning rate, soot shell morphology, occurrence of micro-explosions and soot analysis. A conventional fuel oil with low sulphur content(<10 ppm) (FO) was used as a reference fuel for evaluating the combustion behaviour of TPO. The main difference between the fuels were the presence of micro-explosions during the evaporation of pure TPO droplets, where according to the authors [19], the same behaviour as other pyrolysis bio-oils was observed, while the TPO-FO blend (5% by mass of TPO) evaporated smoothly until the droplet extinguished. The authors related the presence of micro-explosions during the evaporation of TPO droplets to the large differences in volatility between the fuel compounds, which reduced the overall burning time, although TPO showed an earlier onset of vaporization than FO. In addition, TPO showed a higher tendency to form soot compared to FO, which was attributed to its aromatic-rich nature. According to Turns [22], the sooting tendency of fuels is lowest to highest in the order of alkanes, alkenes, alkynes and aromatics.

Muelas et al. [19] reported a variable and time-dependent burning rate coefficient for TPO, which varied between 0 and 0.55 mm^2/s for evaporation conditions at 0% O_2. On the other hand, Williams et al. [14] used the suspended droplet technique to determine the value of the burning rate coefficient of TPO, taking into account the carbon residue obtained after evaporation and combustion of a droplet of TPO, so that the corrected burning rate coefficient was 0.75 mm^2/s. Williams et al. [14] also measured the burning rate coefficient for diesel oil (DO) and obtained a value of 0.88 mm^2/s. Since the burning rate coefficients of TPO and DO are close to each other, the enthalpies of vaporization of both fuels have the same characteristics, which have values of 28.19 and 33.54 kJ/mol, respectively [23]. These similarities may lead to the conclusion that both fuels burn in the same way. However, as Muelas et al. [19] have shown, TPO shows a strong tendency to form soot and carbonaceous deposits [14], which are directly related to the asphaltene content in its composition [24].

In the work of Chumpitaz et al. [12], the atomisation quality of TPO and TPO-DO blends was investigated by measuring the representative droplet size at different operating conditions of a 35kW Y-jet atomiser. The representative

Fig. 1 Number of documents found in Scopus for different word combinations associated with the previous liquid combustion process
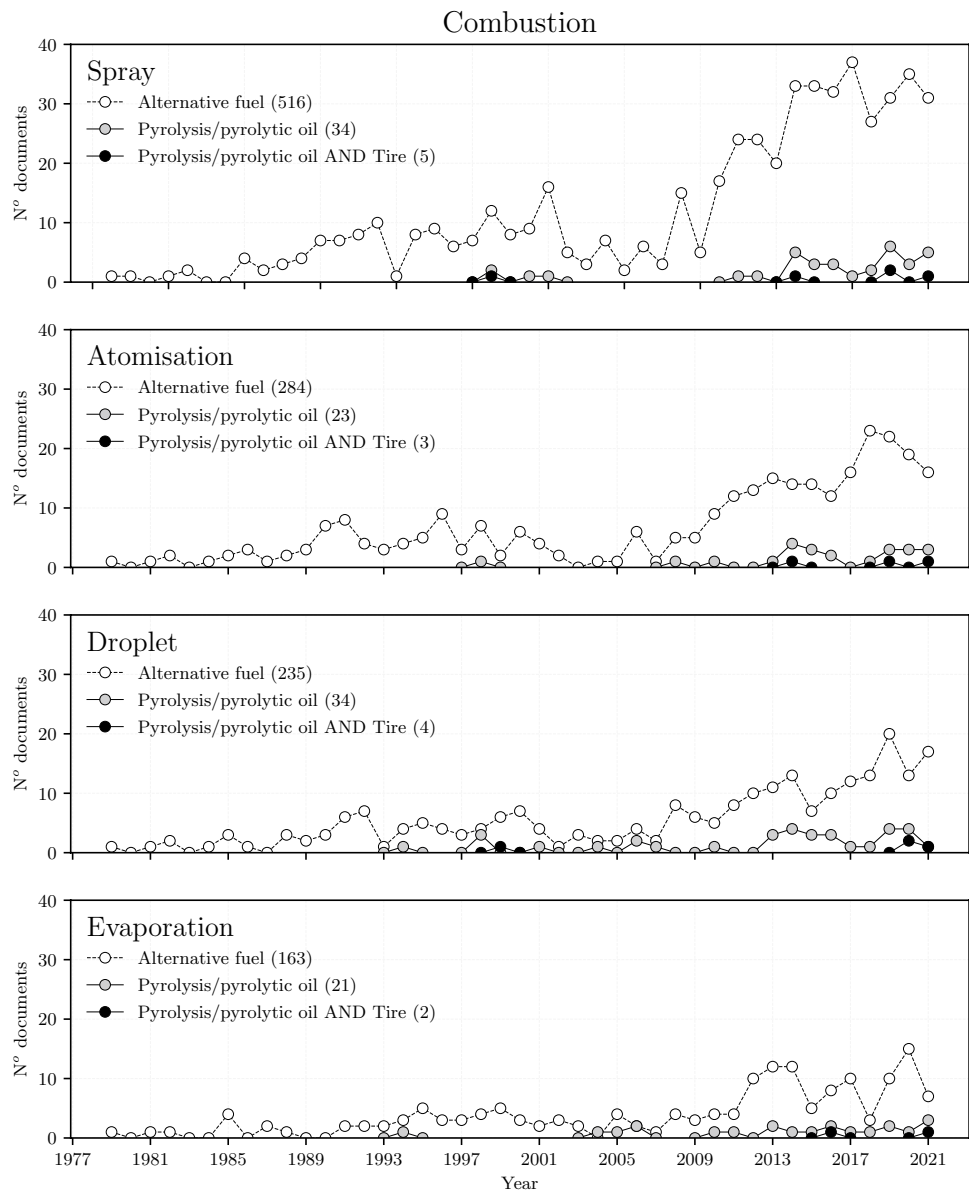
diameters measured were the Sauter mean diameter and mass median diameter using the Malvern Spraytec 2007 laser diffraction system, model STP5936. The authors showed that the Y-jet atomiser, operating at air-fuel mass ratios (AFR) between 0.105 and 0.125 can achieve Sauter mean diameter values of 78 to 40 µm and 68 to 22 µm for TPO-DO blends containing 2 and 10% TPO, respectively, whose values were close to those measured for diesel, between 70 and 40 µm under the same atomisation conditions. However, evaluating the atomisation quality by measuring representative diameters alone hides information about the droplet size distribution of the spray, which is crucial for simulating spray evaporation and combustion.

Therefore, this work aims to evaluate the atomisation quality of TPO and blends with DO by determining the distribution parameters of the density function describing the droplet size distribution of fuel sprays. The distribution parameters are calculated from experimental data obtained from direct measurements of TPO-DO sprays produced with a 35 kW Y-nozzle atomiser. Furthermore, the evaporation of the TPO spray is simulated using the calculated distribution parameters and the influence of the uniformity of the spray on the evaporation is evaluated. This work aims to deepen the knowledge of the atomisation properties of unconventional fuels to reveal their future as alternative fuels.

2 Materials and methods

2.1 Fuels

The sample of tire pyrolysis oil (TPO) was donated by the Brazilian company POLIMIX, which has a capacity to recycle 85 tonnes of tires per day that are recycled in a continuous pyrolysis process (rotating reactors) to produce carbon black, TPO and steel [25]. Meanwhile, diesel oil (DO) was purchased from Shell, marketed under the name Shell Evolux Diesel S-10 (sulphur content less than 10 ppm). TPO-DO blends were prepared to evaluate the influence of TPO on the atomisation quality of the fuel blend. The blends were designated as 2%TPO, 5%TPO, 10%TPO to indicate the blends with 2, 5, and 10% mass fraction of TPO, respectively. The characterization of TPO and DO is described in detail in Chumpitaz et al. [12], as is the equipment used. Table 1 shows a summary of the measured properties of the fuels.

Empirical expressions for estimating density, kinematic viscosity, surface tension, and high heating value of TPO-DO blends have already been published by the authors of this work [3].

2.2 Experimental bench

The experimental bench and dimensions of the Y-nozzle atomiser have been described in detail in a previously published article [12]. Malvern Spraytec's laser diffraction system, model STP5936, was used to measure the representative diameters of the fuel spray jets. This device uses Mie and Fraunhofer theory, depending on the properties of the atomised liquid. Since TPO is an opaque liquid, the Fraunhofer theory was used in this work. The system has a He-Ne laser with a bean wavelength of 632.8 nm. The laser bean has a diameter of 10 mm, which individualises a cylindrical area containing the droplets of fuel spray that are analysed. Figure 2 shows the data acquisition procedure, the operating conditions of the Y-jet atomiser and the two representative diameters measured in this work,

Table 1 Properties of TPO and DO [12]

Properties	TPO	DO
Density at 20 °C [kg/m$_3$]	920.70	830.19
Kinematic viscosity at 25 °C [cSt]	5.10	3.73
Surface tension at 24 °C [mN/m]	28.09	26.00
High heating value [MJ/kg]	42.02	45.30[a]

[a]Gamboa et al. [3]

- Sauter mean diameter (x_{32}), diameter of a droplet whose surface-to-volume ratio is equal to that of the entire spray.
- Mass median diameter (x_{MMD}), diameter of a droplet below (or above) which 50% of the total mass (or volume) of droplets lies [26].

An air-fuel mass ratio (AFR) of above 0.05 was chosen because this AFR allows stable x_{32} and x_{MMD} values to be obtained over a wide range of atomiser operation [27]. The length of the laser path is entered into the Spraytec system, which is determined from the spray cone angle [12] and the distance between atomiser outlet and the laser (100 mm). The measurement performed with the Spraytec system is a continuous measurement, as the fuel spray under investigation corresponds to that produced in furnaces and boilers. This type of measurement allows the system to obtain measurements with a frequency of 1 Hz, i.e. one measurement every second. The measurements of x_{32} and x_{MMD} provided by the device correspond to the average of the values obtained in each test, which lasted 30 s. x_{32} and x_{MMD} were chosen to standardise the spray droplets because they make it possible to determine the course of the size distribution of the spray droplets and to obtain distribution parameters that are important for analysing the uniformity and evaporation of the spray mist.

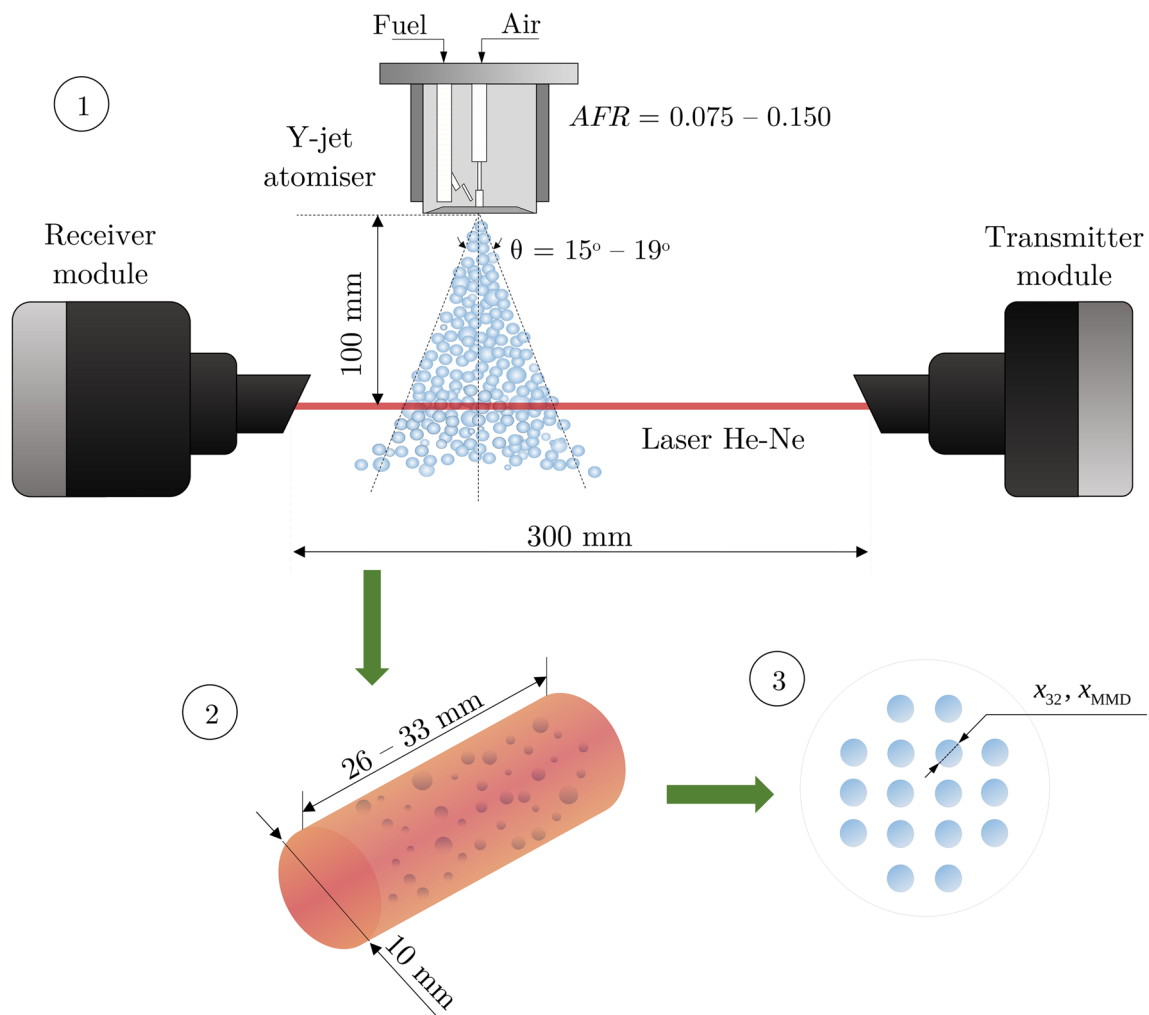### 2.3 Statistical description of the droplet size distribution in a spray

The statistical analysis allows the representation of the distribution of a random variable (droplet diameter) to be represented by distribution parameters such as the mean (μ) and the standard deviation (σ). The description of the droplet size distribution of a spray with only a few statistical parameters thus reduces the problem considerably without losing generality and makes it possible to reconstruct the original size distribution. Moreover, the different representative diameters of the distribution can be determined using these characteristic statistical parameters, which is a significant advantage over representing the spray droplet size by only one representative diameter.

There are several empirical mathematical expressions for describing the droplet size distribution in a spray, such as the equations of Rosin-Ramler, Nukiyama-Tanasawa, Log-Normal, Log-Hyperbolic and Upper Limit [28–32]. Paloposki [33] showed by means of a statistical analysis of χ^2 tests that the Log-Normal distribution functions provided a good fit to the experimental data on the droplet size distribution of liquid sprays, although lower compared to the Nukiyama-Tanasawa and Log-Hyperbolic distribution, but their distribution parameters showed greater mathematical stability and less complexity in determining their values.

1. Spraytec system and Y-jet atomiser; 2. Measurement region; 3. Standardisation of the size of the spray droplet set

Fig. 2 Sequence for obtaining measurements of Sauter mean diameter (x_{32}) and mass median diameter (x_{MMD})

As described above, in was decided in this work to apply the Log-Normal density function (f), Eq. (1),

$$f(y) = \frac{1}{\sigma\sqrt{2\pi}}\exp\left[-\frac{1}{2}\left(\frac{y-\mu}{\sigma}\right)^2\right], \tag{1}$$

in the statistical analysis of the uniformity of TPO and TPO-DO sprays, since it is easy to determine their distribution parameters using only two representative diameters (x_{32} and x_{MMD}). The random variable y is defined on a logarithmic scale to simplify Eq. (1). Experience shows that the mean value μ of the density function in (1) is approximately equal to zero when the variable y is expressed in terms of the droplet diameter (x) and the mass median diameter (x_{MMD}), equation (2).

$$y = \ln\left(\frac{x}{x_{MMD}}\right) \tag{2}$$

On the other hand, the standard deviation σ, in Eq. (1), represents the degree of dispersion or variability of the values of the random variable y. Equation (1) can, however, be rewritten in the form of the uniformity parameter δ according to Eq. (3) and related to the volume of the spray droplets (f_V),

$$f_V(y) = \frac{\delta}{\sqrt{\pi}}\exp\left[-\left(\delta^2 y^2\right)\right], \tag{3}$$

where $\delta = (\sigma\sqrt{2})^{-1}$. It is evident that the smaller the value of the dispersion σ is, the larger will be the uniformity parameter δ of the distribution. Thus, the evaluation of the

uniformity of TPO and TPO-DO sprays is done by comparing the value of δ for each droplet size distribution.

Then, the volume fraction V of droplets with a diameter less than or equal to x is determined by Eq. (4),

$$V = \int_{x_{min}}^{x} f_V(x)\, dx, \tag{4}$$

x_{min} corresponds to the minimum diameter of the spray droplets. From Eq. (4), it is observed that $f_V(x) = dV/dx$ and when $x = x_{max}$ (maximum diameter) $V = 1$ is obtained. Equation (4) can also be written in terms of equation (3) as:

$$V = \int_{x_{min}}^{x} \frac{dV}{dy}\frac{dy}{dx}\, dx = \int_{y_{min}}^{y} f_V(y)\, dy, \tag{5}$$

where $y_{min} = ln(x_{min}/x_{MMD}) < 0$, since $x_{min} < x_{MMD}$. Since the droplets do not have diameters smaller than x_{min} or diameters larger than x_{max}, it results $\int_0^{x_{min}} f_V(x)dx = \int_{-\infty}^{y_{min}} f_V(y)dy = 0$ and $\int_{x_{max}}^{+\infty} f_V(x)dx = \int_{y_{max}}^{+\infty} f_V(y)dy = 0$, respectively, so $\int_{x_{min}}^{x_{max}} f_V(x)dx = \int_{-\infty}^{+\infty} f_V(y)dy = 1$. Consequently, Eqs. (4) and (5) can be expressed according to Eq. (6).

$$V = \int_0^{x} f_V(x)\, dx = \int_{-\infty}^{y} f_V(y)\, dy \tag{6}$$

Furthermore, the representative diameter x_{qp} of order $q + p$ for a distribution of droplets with diameters between x_{min} and x_{max} can be determined using the general definition given by several authors [26, 30, 32], Eq. (7).

$$x_{qp} = \left[\frac{\int_{x_{min}}^{x_{max}} x^{q-3} f_V(x)\, dx}{\int_{x_{min}}^{x_{max}} x^{p-3} f_V(x)\, dx} \right]^{\frac{1}{q-p}} \tag{7}$$

Replacing Eqs. (2) and (3) in (7), and applying a change in the variables, the representative diameter of order $q + p$ for the case of a Log-Normal distribution is obtained, according to Eq. (8),

$$x_{qp} = x_{MMD} \exp\left(\frac{q + p - 6}{4\delta^2} \right) \tag{8}$$

Therefore, the uniformity parameter δ can be calculated from Eq. (8) when x_{MMD} and another representative diameter, such as x_{32} ($q = 3$ and $p = 2$), are measured, which allows the effect of TPO on the quality of TPO-DO spray to be evaluated in terms of droplet size uniformity.

2.4 Evaporation of tire pyrolysis oil spray

The evaporation quality of the TPO spray was evaluated using the d^2-law, according to Eq. (9),

$$\frac{dx^2}{dt} = -K, \tag{9}$$

where x is the droplet diameter at time t. The parameter K is called the burning rate coefficient and depends on properties, such as droplet and evaporation medium density, the transfer number and the mass diffusivity [22]. Muelas et al. [19] reported a time-dependent burning rate coefficient K for TPO that varied between 0 and 0.55 mm^2/s from the start to the burst of the fuel droplet at evaporation conditions with 0% O_2. The micro-explosion of the TPO droplet took place under almost constant K conditions; moreover, the droplet burst prevented the measurement of the solid residue at the end of the evaporation process and the implementation of a correction of the K value. On the other hand, Williams et al. [14] determined the K value for TPO using the suspended droplet technique at room temperature and introduced a correction factor in the case of TPO due to the rapid mass loss (high volatility) and the carbon residue at the end of the TPO droplet combustion. The value given by the authors [14] for TPO was 0.75 mm$^2/s$, which was constant because the transient heating period of the droplet was neglected until temperatures near the boiling point were reached.

Although Eq. (9) ideally models the evaporation of a single droplet, this equation can be extended to a spray by using the same idea as Tanasawa and Tesima [34], who introduce Eq. (9) into the density function of the spray droplet size distribution with respect to mass. The density function with respect to spray volume, Eq. (3), behaves in the same way as the density function with respect to mass ($f_W(x) = dW/dx$) if a uniform and constant density is assumed for the spray droplets. Therefore, the function f_W can be written as depending on evaporation time by substituting Eq. (9) into (3) and assuming a constant burning rate coefficient, according to Eq. (10).

$$f_W(t) = \frac{\delta}{\sqrt{(x_{t=0}^2 - Kt)\pi}} \exp\left\{ -\delta^2 \left[ln\left(\frac{\sqrt{x_{t=0}^2 - Kt}}{x_{MMD}} \right) \right]^2 \right\} \tag{10}$$

$x_{t=0}$ corresponds to the droplet diameter of the spray before the start of evaporation; therefore, Eq. (10) agrees with Eq. (3) at $t = 0$ and the values of $x_{t=0}$ lie between the integration limits of Eq. (6), i.e. x_{min} and x_{max}. The value of x_{min} changes with the evolution of the evaporation process, since after a time t the droplets with diameters smaller than $\sqrt{Kt}$ will have completely evaporated, defining a new minimum value for the droplet size distribution. Therefore, Eq. (10) can be written generally as in Eq. (11).

Table 2 Operating conditions and measurements of x_{32} and x_{MMD} of the TPO spray

Operating conditions	100% TPO			
Fuel mass flow rate [g/s]	1.75	1.32	1.05	0.88
Air mass flow rate [g/s]	0.13	0.13	0.13	0.13
Fuel pressure [bar]	2.05	1.16	1.14	0.56
Air pressure [bar]	3.46	3.46	3.47	3.46
Air-fuel mass ratio, AFR	0.075	0.100	0.125	0.150
Sauter mean diameter, x_{32} [μm]	33.30	29.00	28.16	24.25
Mass median diameter, x_{MMD} [μm]	67.42	56.16	56.22	48.85

Table 4 Operating conditions and measurements of x_{32} and x_{MMD} of the 5%TPO spray

Operating conditions	5% TPO			
Fuel mass flow rate [g/s]	1.70	1.28	1.05	0.90
Air mass flow rate [g/s]	0.13	0.13	0.13	0.13
Fuel pressure [bar]	1.99	1.76	1.52	1.03
Air pressure [bar]	3.45	3.44	3.44	3.43
Air-fuel mass ratio, AFR	0.080	0.100	0.125	0.150
Sauter mean diameter, x_{32} [μm]	32.20	31.60	29.38	25.79
Mass median diameter, x_{MMD} [μm]	57.82	57.73	54.80	46.54

Table 3 Operating conditions and measurements of x_{32} and x_{MMD} of the 2%TPO spray

Operating conditions	2% TPO			
Fuel mass flow rate [g/s]	1.73	1.28	1.05	0.90
Air mass flow rate [g/s]	0.13	0.13	0.13	0.13
Fuel pressure [bar]	2.98	1.57	1.38	1.08
Air pressure [bar]	3.47	3.44	3.44	3.44
Air-fuel mass ratio, AFR	0.080	0.100	0.125	0.150
Sauter mean diameter, x_{32} [μm]	41.64	34.79	33.80	31.94
Mass median diameter, x_{MMD} [μm]	65.21	51.77	49.07	45.76

Table 5 Operating conditions and measurements of x_{32} and x_{MMD} of the 10%TPO spray

Operating conditions	10% TPO			
Fuel mass flow rate [g/s]	1.73	1.28	1.05	0.90
Air mass flow rate [g/s]	0.13	0.13	0.13	0.13
Fuel pressure [bar]	2.93	1.83	1.31	0.85
Air pressure [bar]	3.62	3.52	3.52	3.52
Air-fuel mass ratio, AFR	0.080	0.100	0.125	0.150
Sauter mean diameter, x_{32} [μm]	37.55	30.76	29.74	24.14
Mass median diameter, x_{MMD} [μm]	72.88	57.45	54.57	44.19

$$\frac{dW}{dt}(x,t) = \frac{\delta}{\sqrt{(x^2 - Kt)\pi}}$$

$$\exp\left\{-\delta^2\left[\ln\left(\frac{\sqrt{x^2 - Kt}}{x_{MMD}}\right)\right]^2\right\}, \sqrt{Kt} < x < x_{max} \quad (11)$$

Equation (11) is an ordinary differential equation that can be solved by numerical integration or by the fourth order Runge–Kutta method to obtain the evolution of the spray evaporation process. Subsequently, the mass fraction of vapour formed W_{evap} can be calculated with Eq. (12).

$$W_{evap}(t) = 1 - W = 1 - \int_{\sqrt{Kt}}^{x_{max}} f_W(x)\, dx \quad (12)$$

3 Results and discussion

3.1 Sauter mean diameter and mass median diameter measurements

Measurements of Sauter mean diameter and mass median diameter of TPO and TPO-DO (2, 5 and 10% TPO) sprays are given in Tables 2, 3, 4 and 5, together with the operating conditions of the 35 kW Y-jet atomiser.

Each test was conducted with a constant air mass flow rate (atomising agent) of 0.13 g/s, which allowed to overcome the fuel injection pressure and a two-fluid operating condition of the Y-jet atomiser to be achieved. Otherwise, the twin fluid atomiser would have functioned only as a pressure atomiser, since the atomisation of the fuel would have been generated mainly by the conversion of pressure energy into kinetic energy and not by the transfer of momentum of the fluids (air and fuel).

Tables 2, 3, 4 and 5 show the air-fuel mass ratios (AFR) used in this work, which ranged from 0.075 to 0.150. For the case of the blends of 2, 5, and 10%TPO, the initial value of AFR was 0.080. This value was not achieved for the 100%TPO, which started at AFR = 0.075. The main reason was the high volatility of the TPO. That difference was indicated with an asterisk in Fig. 5. On the other side, the range of AFR between 0.075 and 0.150 was used because, according to Mullinger and Chigier [27], stable x_{32} and x_{MMD} can be achieved over a wide operating range for AFRs above 0.05. Furthermore, each table shows that x_{32} and x_{MMD} decrease with increasing AFR, indicating an improvement in atomisation efficiency as smaller x_{32}s correspond to a larger spray area (from the droplet set). A similar trend is observed for x_{MMD}.

3.2 Fuel spray uniformity

Of the fuel blends investigated, 100%TPO spray had the lowest values for the Sauter mean diameter for the operating ranges studied (Table 2), which might suggest that the mass median diameters should also be the smallest. However, the experimental evidence showed a different behaviour (Tables 3, 4, 5), i.e. the lowest values for the mass median diameter at AFR = 0.100 and AFR = 0.125 were observed for the blend with the lowest TPO content (2%TPO by mass). In order to compare the mass median diameter and the Sauter mean diameter of the fuel blends and the relationship to spray uniformity, the ratio between these values were plotted as a function of AFR, as shown in Fig. 3.

Figure 3 shows that the 2%TPO spray has the lowest x_{MMD}/x_{32} values, the value of which decreases with increasing AFR. However, the 100%TPO spray has the highest values compared to the other blends, which are almost constant in the operating range of the atomiser. The x_{MMD}/x_{32} values for 5%TPO and 10%TPO are close to each other and are between those of 100%TPO and 2%TPO. From Eq. (2), it can be deduced that, with $x_{MMD}/x_{32} \rightarrow 1$, δ increases indefinitely, and consequently the fuel sprays with greater uniformity (Fig. 3) correspond to those whose x_{MMD}/x_{32} values are closer to 1. To prove this fact, the x_{MMD} and x_{32} values (Tables 2, 3, 4, 5) are used in Eq. (2) to determine the uniformity parameter δ of each spray. The calculated values are shown in Fig. 4.

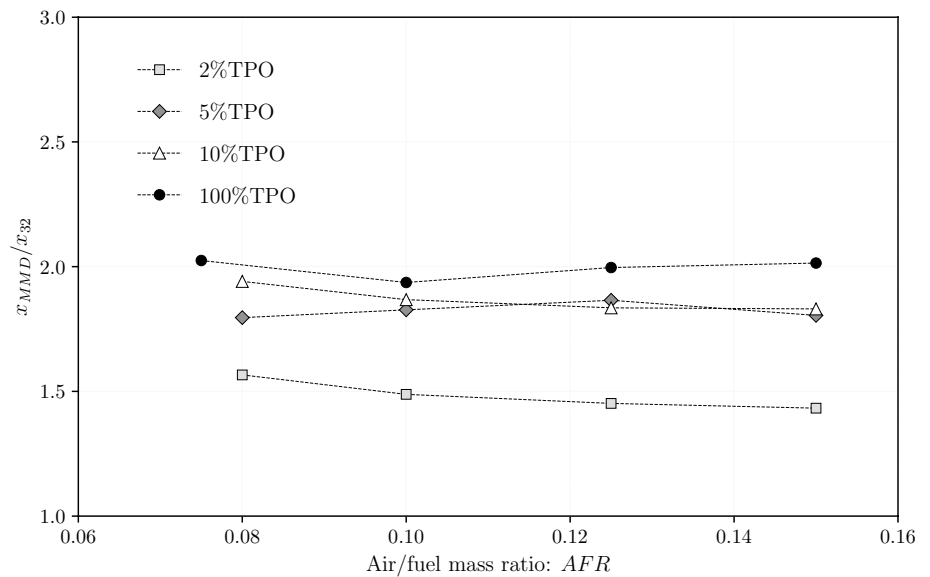**Fig. 3** Ratio of mass median diameter to Sauter mean diameter as a function of AFR

Fig. 4 Uniformity parameter as a function of AFR for TPO-DO sprays
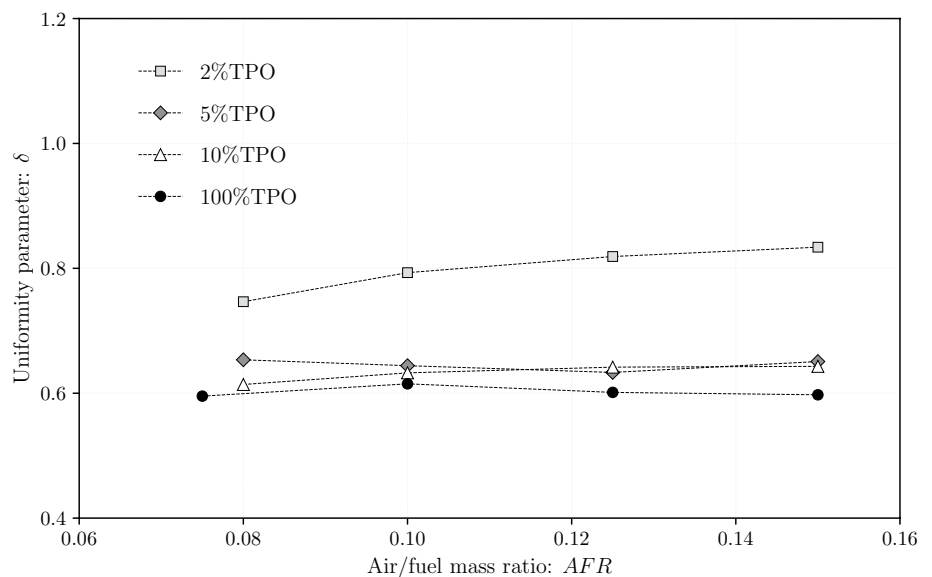
Figure 4 confirms what was discussed above: 2%TPO spray shows the greatest uniformity in droplet size distribution. However, blends containing 5 and 10% TPO show similar droplet size distribution uniformity as 100%TPO. This fact may be related to the higher volatility of TPO compared to diesel, which produces sprays whose droplets lose mass rapidly, resulting in greater variability in droplet sizes. The higher volatility of TPO compared to diesel is evident when comparing their flash points and boiling point ranges: 23 °C and 78–390 °C for TPO, and > 55 °C and 150–370 °C for diesel [19, 35, 36].

Thus, it is not sufficient to evaluate the quality of a spray only on the basis of the Sauter mean diameter, since smaller Sauter mean diameters result from less uniform sprays, which affects the quality of vaporisation and combustion of the fuel spray. Indeed, good atomisation quality results from the combination of a spray of fine droplets with a uniform distribution of the droplets, which promotes vaporisation and subsequent proper mixing with the oxidant to achieve complete combustion of the fuel [37].

3.3 Droplet size distribution of fuel sprays

This section presents the droplet size distributions of fuel sprays in terms of volume, Eqs. (3) and (6). Equation (3) provides a direct visualisation of the fuel spray uniformity level as it uses the dimensionless random variable y defined as $ln(x/x_{MMD})$, which allows all distribution density functions to be represented with a single mean value ($\mu = 0$). However, if the distribution density function were represented as a function of the dimensional random variable x (droplet diameter), the direct identification of the degree of uniformity of the spray would not be as evident as in the first case, since each density function would have its own mean value. To illustrate this fact, Fig. 5 is shown below.

As explained in Sect. 3.2, a smaller Sauter mean diameter (or mass median diameter) does not necessarily mean a more uniform droplet distribution. In Fig. 5a it is not possible to directly determine which spray has a more uniform droplet distribution, but it is possible to see which droplet distribution has the smallest mass median diameter. However, the dimensionless representation of the density function in terms of volume, Fig. 5b, allows direct identification of the more uniform droplet distribution. Using the property that the area under a density function is 1, the curves with the greatest height will be the curves with the smallest base, i.e. with a smaller range of droplet sizes (less variability) and consequently greater uniformity. Therefore, if the uniformity parameter δ were not shown in Fig. 5b, it could be seen from the heights (or bases) of the curves that the droplet distribution of 2%TPO spray has greater uniformity than that of the other fuel sprays (5, 10, and 100%TPO).

The droplet size distribution of fuel sprays (Eqs. (3) and (4)) are shown in Fig. 6, corresponding to different operating conditions (AFR = 0.100, 0.125 and 0.150) of the 35 kW Y-jet atomiser. Equation (3), the cumulative distribution function, is used to observe the volume fractions representing the droplets with the largest diameter in the fuel spray.

Figure 6a, c, e shows the cumulative distribution functions for sprays produced with AFRs of 0.100, 0.125 and 0.150, respectively. In these figures, it can be seen that TPO-DO sprays with TPO mass fractions of 5% or more have a higher proportion of smaller droplets. For example, the volume fractions of droplets less than 15 µm in diameter for the sprays containing 2, 5, 10 and 100% TPO at AFR = 0.100 were 0.082, 0.110, 0.115, and 0.125, respectively, while at AFR = 0.150 they increased to 0.094, 0.149, 0.163, and 0.159. The larger number of smaller diameter droplets in the sprays produced with a high AFR is mainly due to the increase in atomising air velocity (constant air duct diameter), which improves the convective mass transfer of the fuel droplets and the liquid–gas mass transfer exchange. This effect does not only affects smaller droplets, but also the larger ones that are undesirable in spray combustion, as large droplets may not complete their evaporation before reaching the reaction zone (combustion) and may collide with the walls of the combustion chamber, forming carbon deposits and products of incomplete combustion (CO and unburnt hydrocarbons).

In the case of the spray of 2, 5, 10, and 100% TPO, the volume fractions of droplets above 100 µm, $1 - V(x = 100)$, corresponding to AFR = 0.100, were 0.230, 0.308, 0.310, and 0.308, respectively, showing the influence of TPO on the increase in larger droplets in the fuel spray. The Y-jet atomiser operated at a higher AFR produces more uniform sprays and reduces the proportion of larger droplets. At a AFR value of 0.150, the volume fractions of droplets larger than 100 µm for sprays containing 2, 5, 10, and 100% TPO decreased by 22.6, 21.92, 26.19, and 11.50%, respectively, of the value corresponding to the fractions at a AFR value of 0.100. The use of a higher air mass flow rate during atomisation not only improves the quality of the sprays, but also the combustion quality of the TPO-DO blend, which requires high air-fuel ratios to produce stable flames with high flame temperatures and lower emissions (CO and UHC) [38].

On the other hand, Fig. 6b, d, f show how the fuel sprays become more uniform as the AFR increases from 0.100 to 0.150. This is particularly evident in the case of the 2%TPO spray, whose uniformity parameter δ increased from 0.793 to 0.834. The TPO spray exhibits lower uniformity, indicating its high volatility. The high volatility of TPO may be advantageous in the combustion of the fuel spray, as secondary atomisation of the droplets may occur due to droplet microexplosions (disruptive vaporisation) due to the rapid expansion of the volatiles inside, as observed by Muelas et al.

Fig. 5 Density function of **a** dimensional droplet size distribution and **b** dimensionless droplet size distribution a AFR = 0.080
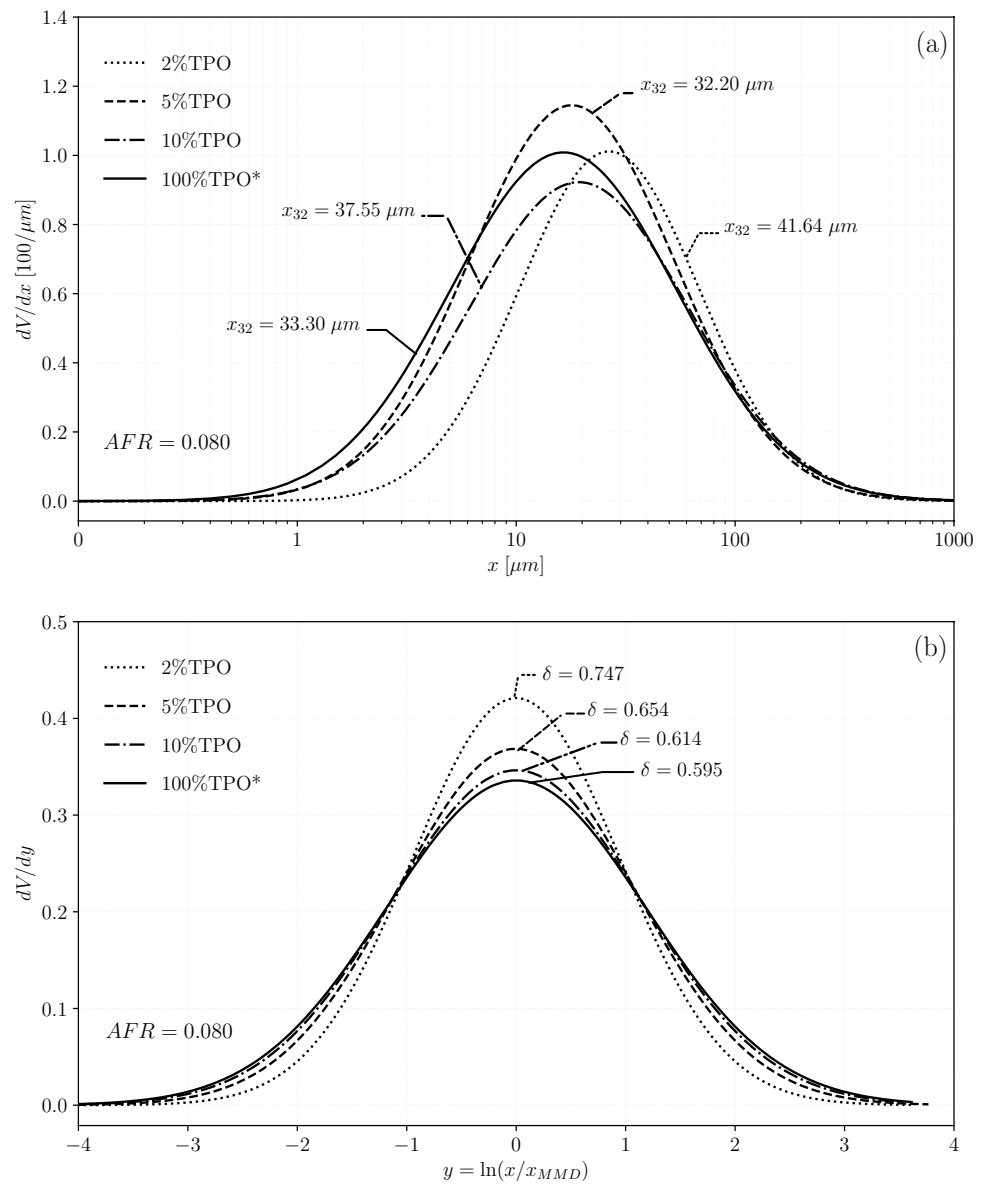
*TPO: spray produced at $AFR = 0.075$

[19]. However, according to Williams [24], multicomponent fuels with a wide range of boiling points (such as TPO) may contain high boiling point components that can thermally decompose, leading to the formation of coke-like residues called cenospheres. The amount of stack solids depends on the asphaltene content of the fuel, which according to Bicakova and Straka [39] is about 4.8% by mass in TPO. These carbonaceous deposits are not only a problem for TPO, but also for other pyrolysis oils, as shown in the comprehensive review by Broumand et al. [37] and Panchasara and Ashwath [40].

Figure 6 shows how proportions of more than 5% TPO in the fuel blend can change the uniformity of the droplet size distribution in a spray, even though TPO and DO have similar physical properties (surface tension and viscosity). According to Wigg's equation [41], the mass median diameter of a spray produced with a twin-fluid atomiser depends mainly on the viscosity and surface tension of the fuel. Therefore, TPO and DO with viscosity of 5.11 and 3.73 cSt and surface tension of 28 and 26 mN/m^2, respectively, at 25 °C produce sprays with a mass median diameter and Sauter mean diameter of similar size, as shown in the previously published work [12]. In agreement with Broumand et al [37], efficient combustion of a liquid fuel requires a sufficiently fine droplet spray with uniform distribution to allow the fuel to vaporise, mix properly with the oxidant and burn completely within the limited residence time and volume of the combustion chamber.
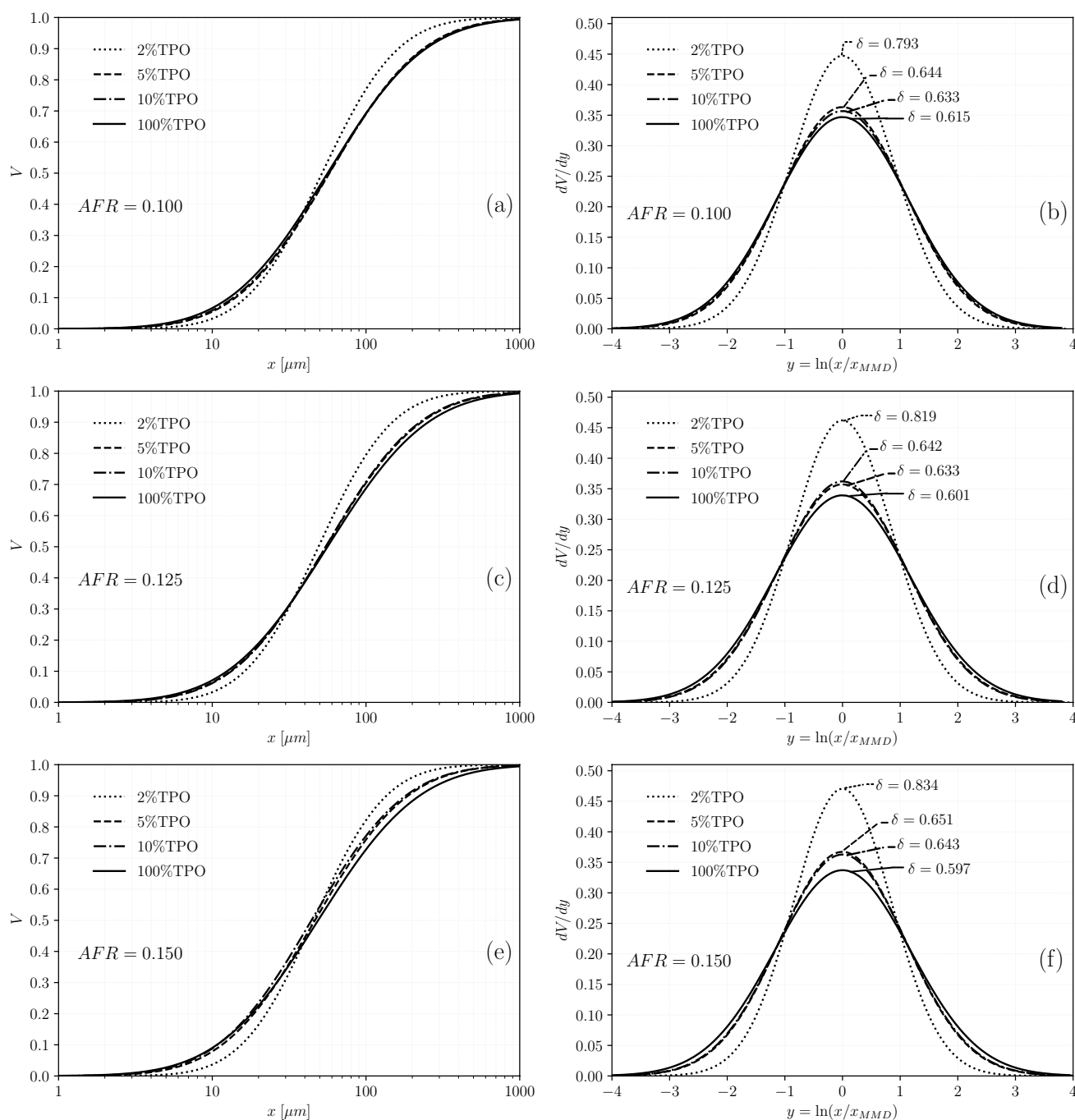
Fig. 6 Droplet size distribution (density function and cumulative distribution function) of fuel spray (2, 5, 10 and 100%TPO) produced by a 35 kW Y-jet atomiser operating at AFR of 0.100 (**a**, **b**), 0.125 (**c**, **d**), and 0.150 (**e**, **f**)

TPO is an excellent candidate as a fuel for generating thermal energy for boilers and furnaces, as it not only has attractive physical properties of atomisation, but also has a high heating value of 42.2 MJ/kg, which allows it to consume similar mass flows as conventional fuels such as diesel (45.2 MJ/kg) [3] to generate similar thermal outputs. Additionally, TPO can be used as a source of chemicals of important commercial value (e.g. D-limonene). However, before it can be used as fuel, TPO needs to be upgraded to reduce the asphaltene and sulphur content so that large carbon residues are not deposited on the walls of the combustion chamber and SO_x emissions are inside acceptable limits. Since TPO has similar properties to diesel oil, the same desulphurisation methods can be applied, i.e. hydrodesulphurisation, desulphurisation by oxidation, extraction, adsorption and precipitation [42].

3.4 Tire pyrolysis oil spray evaporation

The evolution of spray evaporation was determined by solving Eq. (11), assuming a minimum and maximum droplet diameter of 0 and 500 µm, respectively. The maximum diameter of 500 µm was chosen because less than 5% of the spray volume consists of droplets with diameters above this value, as shown in Fig. 7. Furthermore, the maximum diameter chosen is in the range of sizes relevant for combustion applications, i.e. between 5 and 800 µm [43].

It can be seen from Fig. 7 that the cumulative distribution curves for the 100%TPO spray generated at AFR equal to 0.125 and 0.100 overlap, that is, they present a very close droplet size distribution, so they can be expected to show an equal evaporation evolution. However, the cumulative distribution curves of the spray generated at AFR = 0.150 present a lower proportion of larger droplets in relation to the spray generated at 0.075, 0.100 and 0.125. For example, the spray generated at AFR = 0.150 has a volume proportion of droplets greater than 70 µm of 0.381, while for sprays generated at AFR = 0.075, 0.100 and 0.125, this proportion is 0.487, 0.424 and 0.426, respectively.

The spray evaporation simulation was carried out assuming a constant burning rate coefficient of 0.75 mm²/s, the value of which was given by Williams et al. [14], as mentioned in section 2.4. The calculations were performed for TPO only, as the burning rate coefficients of TPO-DO blends could not be found in the literature. Although the burning rate coefficient of diesel is known (0.88 mm²/s), its evaporation simulation was not considered in this analysis because it is directly evident from Eq. (9) that the higher the burning rate coefficient is, the shorter the droplet evaporation time.

However, since TPO is a fuel for which there are few studies on evaporation (Fig. 1), it is more attractive to theoretically evaluate the evolution of spray evaporation using the statistical parameters of uniformity obtained for each AFR in the experimental tests of TPO. Figure 8 shows the results for the TPO spray produced by a 35 kW Y-jet atomiser operating at a AFR of 0.075 to 0.150.

Figure 8 shows how the mass fraction of droplets with diameters smaller than 500 µm in the spray decreases with increasing evaporation time. According to Eq. (9), the mass fraction of droplets with diameters smaller than 500 µm is completely evaporated after a time of 0.33 s. For this reason, the graphs in Fig. 8 appear to be the same, as they were calculated assuming a single x_{max}, but there are slight differences in the amounts of vapour formed during the evaporation time. For example, after a time of 0.001 s for AFRs of 0.075, 0.100, 0.125 and 0.150, the mass fractions of unevaporated sprays are 0.814, 0.791, 0.788, and 0.761, respectively, i.e. the higher the AFR, the greater the mass fraction of evaporated droplets for the same time. As can be seen from Fig. 8a–d that the uniformity parameters do not show significant differences, so the influence of this parameter on the evaporation of TPO cannot be directly state, but it may be associated with the decrease in the proportion of larger droplets as AFR increases (see Fig. 7). Nevertheless, the experiments showed that the Sauter mean diameter for TPO (Table 2) decreased with increasing AFR, indicating a correlation between x_{32} and the mass fraction of the evaporated spray. This fact was already observed by Alkidas [44], who analytically showed that the evaporation properties of polydisperse sprays are more strongly correlated with their initial Sauter mean diameter than with their droplet size

Fig. 7 Analysis region of the 100% TPO spray evaporation simulation
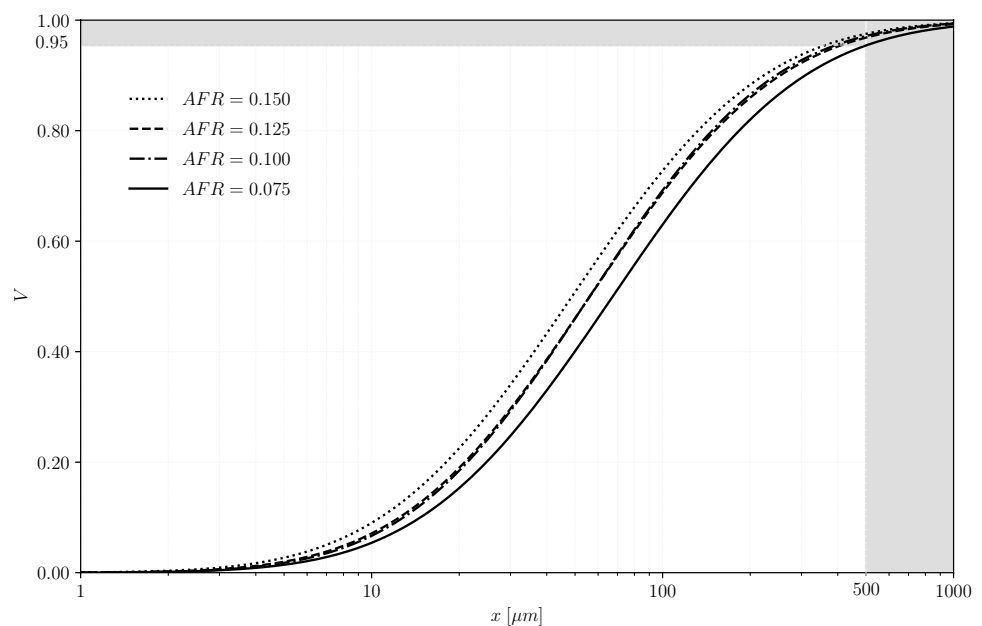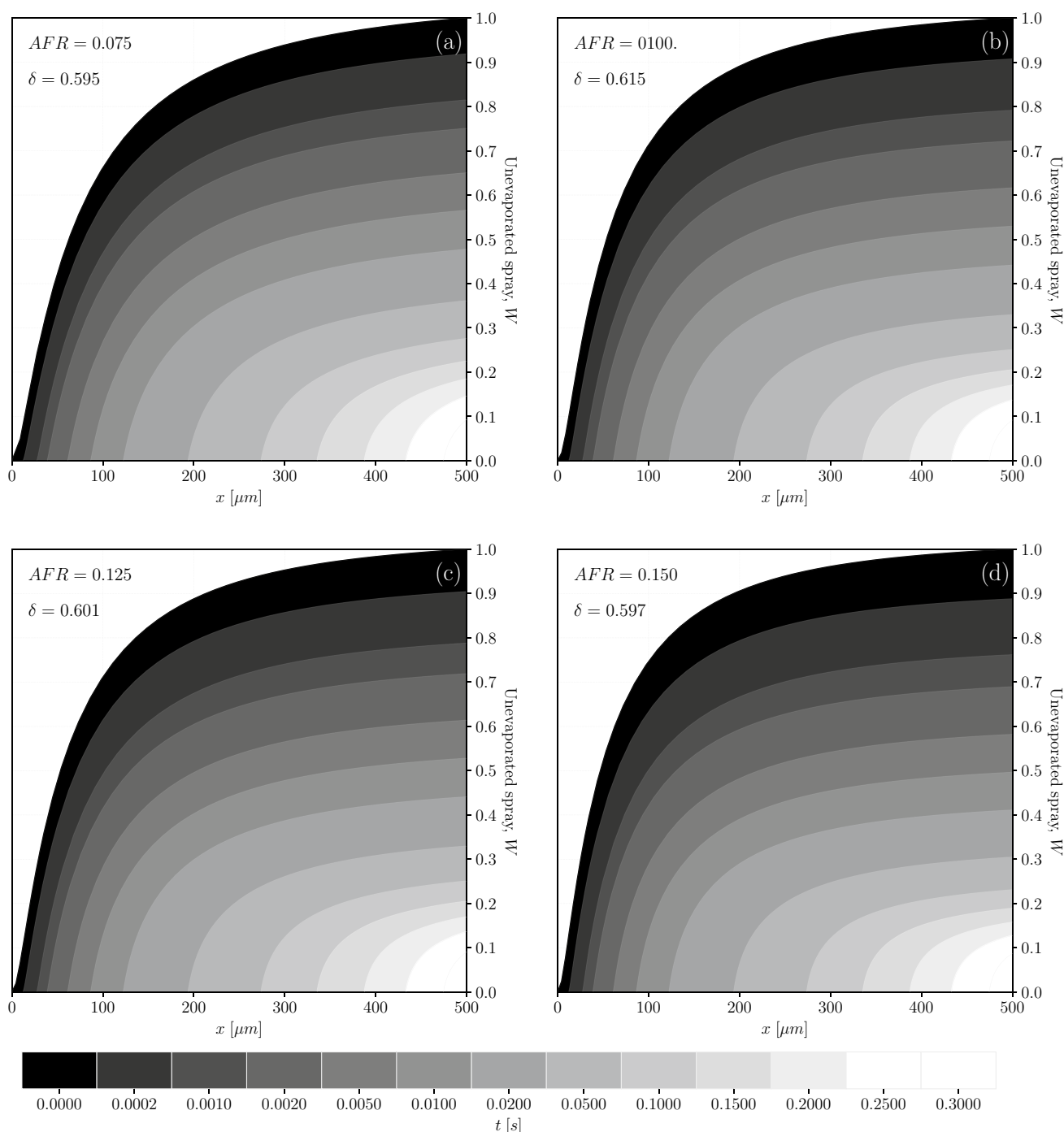
Fig. 8 Mass fraction of unevaporated spray of TPO produced by a 35 kW Y-jet atomiser operating at a AFR of **a** 0.075, **b** 0.100, **c** 0.125, and **d** 0.150

distribution properties. To observe this behaviour, Eq. (12) is used to calculate the evolution of vapour formation as a function of time at different AFRs, Fig. 9.

Figure 9 shows the inverse proportionality between the Sauter mean diameter and the spray evaporation of TPO, illustrating the influence of this representative diameter on the fuel evaporation process. In fact, the influence of droplet

size distribution is embedded in the Sauter mean diameter, as a larger presence of small diameter droplets implies a larger surface area of the droplet system (spray) and consequently a smaller Sauter mean diameter ($x_{32} \sim V_{\text{spray}}/A_{\text{spray}}$). Since AFR affects both the droplet size distribution (Fig. 6) and the Sauter mean diameter (Table 2), different AFR values resulted in different evaporation qualities, as can be seen

Fig. 9 Fraction of vapour formed from the TPO spray as a function of evaporation time at different AFRs
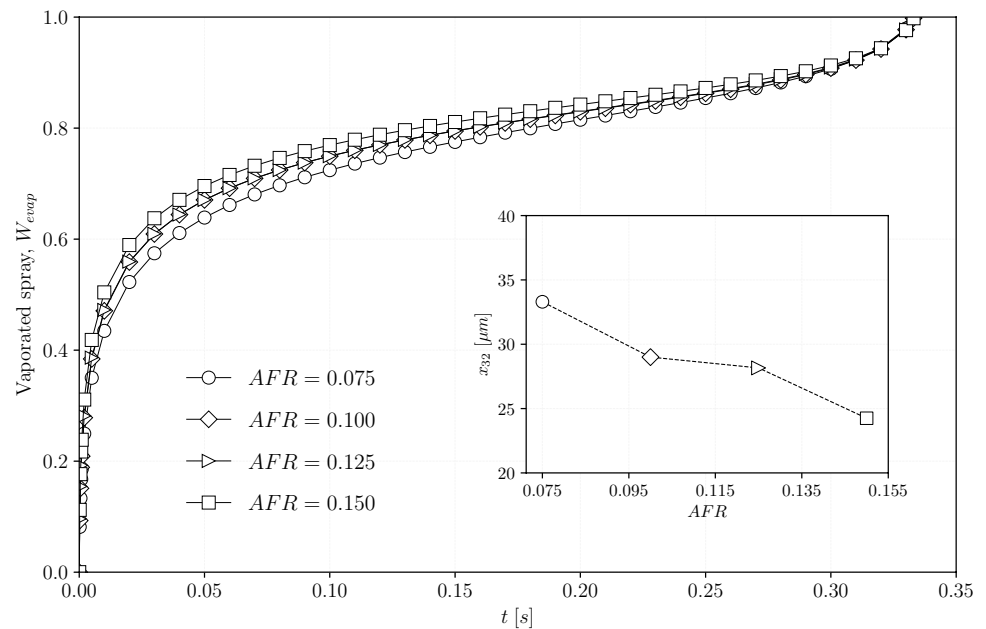
in Fig. 9. This difference becomes more noticeable when comparing the evaporation development of sprays produced with AFR = 0.075 and 0.150. At 0.05 s, for example, the first spray has evaporated 64% of the original spray, the second 70%. Furthermore, it can be seen from Fig. 9 that the evaporation curves of the sprays produced at AFR = 0.100 and 0.125 overlap, so that it is not possible to distinguish between them. This fact is mainly due to the fact that both sprays have similar Sauter mean diameters, 29 and 28.16 µm, respectively. Thus, the Y-jet atomiser with high AFRs (0.150) produces a TPO spray with greater uniformity and smaller Sauter mean diameters, which promotes the vaporisation of a greater percentage of the spray, which improves combustion conditions as more fuel vapour reaches the reaction zone and releases greater heat energy that contributes to the faster vaporisation of the remaining droplets.

4 Conclusions

A theoretical–experimental study based on statistical techniques was conducted to evaluate the atomisation and evaporation of TPO and blends with diesel oil. A Log-Normal density function was used to model the droplet size distribution of fuel sprays produced by a 35 kW Y-jet twin-fluid atomiser. The uniformity parameters of the density function associated with each fuel spray were evaluated as a function of the atomiser operating conditions (AFR from 0.075 to 0.150). High AFR values showed improvements in the atomisation quality of the fuel blends increased the uniformity of the spray and decreased the Sauter mean diameter. However, mass fractions above 5% TPO in the fuel blend reduced the uniformity of the spray

and increased the occurrence of droplets with diameters above 100 µm.

In addition, the evaporation of the TPO spray was evaluated using the d^2-law integrated into the Log-Normal density function. In simulating the evaporation of the TPO spray produced by the Y-jet atomiser at a AFR in the range of 0.075 to 0.150, droplet diameters of up to 500 µm were assumed. Increasing the AFR from 0.075 to 0.150 resulted in an improvement in spray evaporation due to a reduction in the Sauter mean diameter and an increase in the volume fractions of smaller droplets. High quality atomisation of TPO is not sufficient if no sulphur reduction is carried out, even if the TPO is used as fuel in furnaces and boilers. The sulphur content not only damages the injection systems of combustion equipment but also generates emissions of sulphur oxides which are harmful to the health of living beings. The future of TPO as an alternative fuel depends entirely on the application of effective methods to reduce these sulphur-containing components without significantly changing its energetic (calorific value) and physical (surface tension, viscosity and density) properties.

References

1. World Business Council for Sustainable Development (2020) Global ELT Management-A global state of knowledge on

collection rates, recovery routes, and Managements Methods. http://docs.wbcsd.org. Accessed 29 March 2022

2. Instituto Brasileiro do Meio Ambiente e dos Recursos Naturais Renováveis (2022) Relatório de Pneumáticos 2021. http://www.ibama.gov.br. Accessed 04 November 2022

3. Gamboa AR, Rocha AM, dos Santos LR, de Carvalho JA (2020) Tire pyrolysis oil in Brazil: potential production and quality of fuel. Renew Sustain Energy Rev 120:109614. https://doi.org/10.1016/j.rser.2019.109614

4. Menares T, Herrera J, Romero R, Osorio P, Arteaga-Pérez LE (2020) Waste tires pyrolysis kinetics and reaction mechanisms explained by TGA and Py-GC/MS under kinetically-controlled regime. Waste Manag 102:21–29. https://doi.org/10.1016/j.wasman.2019.10.027

5. Song Z, Liu L, Yang Y, Sun J, Zhao X, Wang W, Mao Y, Yuan X, Wang Q (2018) Characteristics of limonene formation during microwave pyrolysis of scrap tires and quantitative analysis. Energy 142:953–961. https://doi.org/10.1016/j.energy.2017.10.101

6. Sharma SK, Das RK, Sharma A (2016) Improvement in the performance and emission characteristics of diesel engine fueled with jatropha methyl ester and tyre pyrolysis oil by addition of nano additives. J Braz Soc Mech Sci Eng 38:1907–1920. https://doi.org/10.1007/s40430-015-0454-x

7. Vieira FR, Luna CR, Arce GF, Avila I (2020) Optimization of slow pyrolysis process parameters using a fixed bed reactor for biochar yield from rice husk. Biomass Bioenergy 132:105412. https://doi.org/10.1016/j.biombioe.2019.105412

8. Canettieri EV, da Silva VP, Neto TGS et al (2018) Physicochemical and thermal characteristics of sugarcane straw and its cellulignin. J Braz Soc Mech Sci Eng 40:416. https://doi.org/10.1007/s40430-018-1331-1

9. Neves D, Thunman H, Matos A, Tarelho L, Gómez-Varea A (2011) Characterization and prediction of biomass pyrolysis products. Prog Energy Combust Sci 37(5):611–630. https://doi.org/10.1016/j.pecs.2011.01.001

10. Neves D, Thunman H, Matos A, Tarelho L, Gómez-Varea A (2010) Empirical correlations for biomass predictions. In: 18th European biomass conference and exhibition, pp 1055-1062. https://doi.org/10.5071/18thEUBCE2010-VP2.3.32

11. Gamboa AR (2020) Viability study of production and atomization of tire pyrolysis oil in Brazil. Thesis, São Paulo State University. http://hdl.handle.net/11449/193602

12. Chumpitaz GRA, Coronado CJR, Carvalho JA et al (2019) Design and study of a pure tire pyrolysis oil (TPO) and blended with Brazilian diesel using Y-Jet atomizer. J Braz Soc Mech Sci Eng 41:139. https://doi.org/10.1007/s40430-019-1632-z

13. Das RK, Sharma SK (2017) Fuel characterization and performance parameters analysis of diesel engine using blends of palm biodiesel and tyre pyrolysis oil. J Braz Soc Mech Sci Eng 39:1491–1497. https://doi.org/10.1007/s40430-016-0696-2

14. Williams PT, Bottrill RP, Cunliffe AM (1998) Combustion of tyre pyrolysis oil. Process Saf Environ Prot 76(4):291–301. https://doi.org/10.1205/095758298529650

15. Contreras RG, Martínez JD, Armas O, Murillo R, García T (2016) Study of a residential boiler under start-transient conditions using a tire pyrolysis liquid (TPL)/diesel fuel blend. Fuel 158:744–752. https://doi.org/10.1016/j.fuel.2015.06.046

16. Gamboa AR, de Carvalho JA, Rocha AM (2017) Calculation of tyre pyrolytic oil combustion products using the method of Gibbs free energy minimization. IEEE Lat Am Trans 15(6):1078–1083. https://doi.org/10.1109/TLA.2017.7932695

17. Dogan O, Çelik MB, Ozdalyan B (2012) The effect of tire derived fuel/diesel fuel blends utilization on diesel engine performance

18. Sharma A, Murugan S (2015) Potential for using a tyre pyrolysis oil-biodiesel blend in a diesel engine at different compression ratios. Energy Convers Manag 93:289–297. https://doi.org/10.1016/j.enconman.2015.01.023

19. Muelas A, Callén MS, Murillo R, Ballester J (2019) Production and droplet combustion characteristics of waste tire pyrolysis oil. Fuel Process Technol 196:106149. https://doi.org/10.1016/j.fuproc.2019.106149

20. Nursal RS, Khalid A, Abdullah IS, Jaat N, Darlis N, Koten H (2021) Autoignition behavior and emission of biodiesel from palm oil, waste cooking oil, tyre pyrolysis oil, algae and jatropha. Fuel 306:121695. https://doi.org/10.1016/j.fuel.2021.121695

21. Seljak T, Opresnik SR, Katrasnik T (2014) Microturbine combustion and emission characterization of waste polymer-derived fuels. Energy 77:226–234. https://doi.org/10.1016/j.energy.2014.07.020

22. Turns S (2012) An introduction to combustion: concepts and applications. New York

23. Umeki ER, de Oliveira CF, Torres RB, dos Santos RG (2016) Physico-chemistry properties of fuel blends composed of diesel and tire pyrolysis oil. Fuel 185:236–242. https://doi.org/10.1016/j.fuel.2016.07.092

24. Williams A (1990) Combustion of liquids fuel sprays. Leeds

25. Polimix (2022) Polimix Ambiental. http://www.polimix.com.br. Accessed 29 March 2022

26. Lefebvre AH, McDonell VG (2017) Atomization and sprays. Boca Raton

27. Mullinger PJ, Chigier NA (1974) The design and performance of internal mixing multijet twin fluid atomizers. J Inst Fuel 47(43):251–261

28. Vesilind P (1980) The Rosin-Ramler particle size distribution. Resour Recover Conserv 5(3):275–277. https://doi.org/10.1016/0304-3967(80)90007-4

29. Nukiyama S, Tanasawa Y (1939) Experiments on the atomization of liquids in an air stream. Trans Soc Mech Eng (Japan) 5(18):62–67

30. Mugele R, Evans H (1951) Droplet size distribution in sprays. Ind Eng Chem 43(6):1317–1324. https://doi.org/10.1021/ie50498a023

31. Bhatia JC, Durst F. Description of sprays using joint hyperbolic distribution in particle size and velocity. Combust Flame 81:203–218. https://doi.org/10.1016/0010-2180(90)90019-N

32. Ashgriz N (2011) Handbook of atomization and sprays. Theory and applications. New York

33. Paloposki T (1994) Drop size distributions in liquid sprays. Acta Polytechnica Scandinavica Mech Eng Ser 36:114

34. Tanasawa Y, Tesima T (1958) On the theory of combustion rate of liquid fuel spray. Bull JSME 1(1):36–41. https://doi.org/10.1299/jsme1958.1.36

35. Ayanoglu A, Yumrutas R (2016) Rotary kiln and batch pyrolysis of waste tire to produce gasoline and diesel like fuels. Energy Convers Manag 111:261–270. https://doi.org/10.1016/j.enconman.2015.12.070

36. Rodriguez IM, Laresgoiti MF, Cabrero MA, Torres A, Chomón MJ, Caballero B (2001) Pyrolysis of scrap tyres. Fuel Process Technol 72(1):9–22. https://doi.org/10.1016/S0378-3820(01)00174-6

37. Broumand M, Green SA, Yun S, Hong Z, Thomson MJ (2020) Spray combustion of fast pyrolysis bio-oils: applications, challenges, and potential solutions. Prog Energy Combust Sci 79:100834. https://doi.org/10.1016/j.pecs.2020.100834

38. Pilusa J, Muzenda E. Combustion characteristics of waste tyre pyrolysis fuel as industrial burner fuel. Developments in Combustion Technology, In: Kyprianidis KG, Skvaril J (ed) Developments

in combustion technology. IntechOpen, London, pp 98–115. https://doi.org/10.5772/63078

39. Bicaková O, Straka P (2016) Co-pyrolysis of waste tire/coal mixtures for smokeless fuel, maltenes and hydrogen-rich gas production. Energy Convers Manag 116:203–213. https://doi.org/10.1016/j.enconman.2016.02.069

40. Panchasara H, Ashwath N (2021) Effect of pyrolysis Bio-oils on fuel atomization—a review. Energies 14:794. https://doi.org/10.3390/en14040794

41. Wigg LD (1964) Drop size prediction for twin-fluid atomizers. J Inst Fuel 27:500–505

42. Serefentse R, Ruwona W, Danha G, Muzenda E (2019) A review of the desulphurization methods used for pyrolysis oil. Procedia Manuf 35:762–768. https://doi.org/10.1016/j.promfg.2019.07.013

43. McCreath CG, Beér JM (1976) A review of drop size measurement in fuel sprays. Appl Energy 2(1):3–15. https://doi.org/10.1016/0306-2619(76)90036-2

44. Alkidas AC (1981) The influence of size distribution parameters on the evaporation of polydisperse dilute sprays. Int J Heat Mass Transf 24(12):1913–1923. https://doi.org/10.1016/0017-9310(81)90114-9